Brain Advance Access published December 6, 2013

doi:10.1093/brain/awt325 Brain 2013: Page 1 of 12 | 1

BRAIN
A JOURNAL OF NEUROLOGY

Pantethine treatment is effective in recovering the disease phenotype induced by ketogenic diet in a pantothenate kinase-associated neurodegeneration mouse model

Dario Brunetti,[1] Sabrina Dusi,[1] Carla Giordano,[2] Costanza Lamperti,[1] Michela Morbin,[3] Valeria Fugnanesi,[3] Silvia Marchet,[1] Gigliola Fagiolari,[4] Ody Sibon,[5] Maurizio Moggio,[4] Giulia d'Amati[2] and Valeria Tiranti[1]

1 Unit of Molecular Neurogenetics, Foundation IRCCS Neurological Institute C. Besta, Milan, Italy
2 Department of Radiology, Oncology and Pathology, Sapienza University, Policlinico Umberto I, Rome, Italy
3 Unit of Neuropathology and Neurology, Foundation IRCCS Neurological Institute C. Besta, Milan, Italy
4 Unit of Neuromuscular and Rare Disorders, Foundation IRCCS Ca' Granda Ospedale Maggiore Policlinico, Department of Neurological Sciences, Milan, "Dino Ferrari" Centre, Milan University, Italy
5 Department of Cell Biology, University Medical Centre Groningen, University of Groningen, The Netherlands

Correspondence to: Valeria Tiranti,
Unit of Molecular Neurogenetics,
IRCCS Foundation Neurological Institute "C. Besta",
Via Temolo, 4,
20126 Milan, Italy,
E-mail: tiranti@istituto-besta.it

Pantothenate kinase-associated neurodegeneration, caused by mutations in the *PANK2* gene, is an autosomal recessive disorder characterized by dystonia, dysarthria, rigidity, pigmentary retinal degeneration and brain iron accumulation. *PANK2* encodes the mitochondrial enzyme pantothenate kinase type 2, responsible for the phosphorylation of pantothenate or vitamin B5 in the biosynthesis of co-enzyme A. A *Pank2* knockout (*Pank2*$^{-/-}$) mouse model did not recapitulate the human disease but showed azoospermia and mitochondrial dysfunctions. We challenged this mouse model with a low glucose and high lipid content diet (ketogenic diet) to stimulate lipid use by mitochondrial beta-oxidation. In the presence of a shortage of co-enzyme A, this diet could evoke a general impairment of bioenergetic metabolism. Only *Pank2*$^{-/-}$ mice fed with a ketogenic diet developed a pantothenate kinase-associated neurodegeneration-like syndrome characterized by severe motor dysfunction, neurodegeneration and severely altered mitochondria in the central and peripheral nervous systems. These mice also showed structural alteration of muscle morphology, which was comparable with that observed in a patient with pantothenate kinase-associated neurodegeneration. We here demonstrate that pantethine administration can prevent the onset of the neuromuscular phenotype in mice suggesting the possibility of experimental treatment in patients with pantothenate kinase-associated neurodegeneration.

Keywords: pantothenate kinase-associated neurodegeneration (PKAN); mitochondria; ketogenic diet; pantethine

Abbreviation: PKAN = pantothenate kinase-associated neurodegeneration

Received July 19, 2013. Revised September 6, 2013. Accepted October 5, 2013.

Introduction

The common feature of a group of genetic disorders, termed neurodegeneration with brain iron accumulation, is brain iron overload identified by radiological and histopathological examinations (Kruer *et al.*, 2012). Different subtypes of neurodegeneration with brain iron accumulation have been defined at the genetic level but pantothenate kinase-associated neurodegeneration (PKAN) syndrome is the most frequent form.

PKAN is caused by mutations in the *PANK2* gene, which codes for the mitochondrial enzyme pantothenate kinase 2. This enzyme is involved in the co-enzyme A biosynthetic pathway, catalysing the phosphorylation of vitamin B5 or pantothenate (Hayflick, 2003). PKAN usually manifests in childhood with gait disturbances and rapidly progresses to a severe movement deficit with dystonia, dysarthria and dysphagia. The hallmark of this disease is the eye-of-the-tiger signal in the globus pallidus on T_2-weighted MRI (Hayflick *et al.*, 2003; Gregory *et al.*, 2009)

To date, the mechanistic connection linking PANK2 dysfunction, neurodegeneration and alteration of iron homeostasis has not been understood, thus preventing our comprehension of the pathogenesis of the disease and the design of efficient therapeutic strategies. It has been proposed that reduced PANK2 enzymatic activity determines the accumulation of cysteine, which may chelate iron thus promoting the formation of free radicals (Gregory *et al.*, 2008); alternatively, defects in co-enzyme A and, as a consequence, in phospholipid metabolism may damage the membranes and lead to increased oxidative stress, which may alter iron homeostasis (Leonardi *et al.*, 2007).

The mouse models of PKAN display incomplete phenotypes, including hardly any brain iron accumulation. *Pank2*$^{-/-}$ mice show growth reduction, retinal degeneration, male infertility because of azoospermia (Kuo *et al.*, 2005), and mitochondrial dysfunctions (Brunetti *et al.*, 2012) under standard diet conditions. Retinal degeneration (Kuo *et al.*, 2005) was not confirmed in a recent *Pank2* knockout mouse (Garcia *et al.*, 2012) and this phenotype is uncertain. A movement disorder was present in mice on a pantothenic acid-deficient diet (Kuo *et al.*, 2007). A *Pank1* knockout mouse (Leonardi *et al.*, 2010) displayed a metabolic disorder characterized by altered fatty acid oxidation and gluconeogenesis, causing mild hypoglycaemia. An additional mouse model consisting of a double *Pank1/Pank2* knockout (Garcia *et al.*, 2012) showed a severe phenotype characterized by hypoglycaemia and hyperketonaemia leading to dysfunctional post-natal development and premature death at 17 days.

Based on the role of co-enzyme A in several crucial cellular metabolic pathways, we tested the hypothesis to stress the *Pank2*$^{-/-}$ mouse model with a high-fat ketogenic diet. Ketone bodies produced by the ketogenic diet through fatty acid oxidation bypass glycolysis and enter the citric acid cycle to produce oxidative phosphorylation (OXPHOS) substrate. Mice on a ketogenic diet use mainly fatty acid oxidation and OXPHOS for ATP production as compared to mice on a standard diet (Laffel, 1999). We observed that only ketogenic diet-fed *Pank2*$^{-/-}$ mice presented typical signs of neurological and motor impairment, as well as neuropathological findings, resembling the phenotype observed in patients with PKAN. Moreover, these mice showed muscular dysfunctions with mitochondrial morphological alterations, which were also detected in the muscle of a patient with PKAN.

Recently, a PANK2 knockout *Drosophila* model has shown that panthethine can serve as a compound to bypass the block due to severe impairment of pantothenate kinase and that it is able to rescue brain degeneration, mitochondrial dysfunction and locomotor disabilities (Rana *et al.*, 2010).

To determine if pantethine was able to counteract the disease phenotype elicited in ketogenic diet-fed *Pank2*$^{-/-}$ mice, we continuously administered pantethine in drinking water during the ketogenic treatment. Our data indicated that pantethine treatment was safe, with no side effects and was able to ameliorate both the majority of the symptoms in the nervous and muscular systems and the morphological features of neuronal and mitochondrial damage.

Materials and methods

Animals and diets

Animal studies were approved by the Ethics Committee of the Foundation IRCCS Neurological Institute C. Besta, in accordance with guidelines of the Italian Ministry of Health: Project no. BT4/2011. The use and care of animals followed the Italian Law D.L. 116/1992 and the EU directive 86/609/CEE.

Standard diet (Mucedola), ketogenic diet (E15149-30, ssniff Spezialdiaten) and water were given *ad libitum*. Ketogenic diet composition: 79.2 % fat; 8% protein; 5% crude fibre; 4.5 % crude ash; 0.6% starch; 0.7% sugar (31.6 MJ/kg), with multi-vitamin addition. Pantethine (Sigma) was administered at a concentration of 15 mg/kg/day in drinking water. The JM129/SvJ-C57BL/6 *Pank2*$^{+/-}$ mice used in this study were kindly provided by Professor Hayflick (Kuo *et al.*, 2005).

Animals were housed two or three in a cage, in a temperature-controlled (21°C) room with a 12 h light-dark cycle and ~60% relative humidity.

The experimental design included four groups of mice: (i) the 'standard diet' group composed of eight *Pank2*$^{-/-}$ mice (four male and four female) and nine *Pank2*$^{+/+}$ (five male and four female) on a standard diet for 2 months; (ii) the 'standard diet + pantethine' group composed of eight *Pank2*$^{-/-}$ mice (four male and four female) and 12 *Pank2*$^{+/+}$ (five male and seven female) on a standard diet with the concomitant administration of pantethine for 2 months; (iii) the 'ketogenic diet' group composed of 20 *Pank2*$^{-/-}$ mice (nine male and 11 female) and 26 *Pank2*$^{+/+}$ (11 male and 15 female) on an *ad libitum* ketogenic diet for 2 months; and (iv) the 'ketogenic diet + pantethine' group composed of 13 *Pank2*$^{-/-}$ mice (five male and eight female) and 16 *Pank2*$^{+/+}$ (five male and 11 female) on an *ad libitum* ketogenic diet with the concomitant administration of pantethine.

Behavioural and motor skills analysis

The different groups were monitored weekly for onset of postural abnormalities, loss of weight and general behavioural changes. We detected spontaneous motor activity over a continuous period of 15 h (at any time between 17:00 pm and 08:00 am) in an activity cage (Ugo Basile) for four single-gender groups of 3-month-old *Pank2*$^{+/+}$ and *Pank2*$^{-/-}$ mice, each comprising three mice of each genotype. In total 12 *Pank2*$^{+/+}$ and 12 *Pank2*$^{-/-}$ mice were analysed.

Measure of motor exercise endurance was evaluated using a treadmill apparatus (Columbus Instruments) counting the number of falls in the motivational grid during a gradually accelerating program with speed initially at 3.8 m/min and increasing by 3 m/min every 2 min. The test was terminated by exhaustion, defined by >10 falls/min into the motivational grid.

A footprint test was performed by painting hindlimbs with non-toxic ink and placing mice at one end of an enclosed, dark tunnel on white paper. Mice walked along a 28 cm long, 7 cm wide strip; stride length and width of consecutive steps were measured. These tests were carried out in 3-month-old mice to monitor the phenotype.

Histology, histochemistry and immunohistochemistry

Histological, histochemical and immunohistochemical analyses were performed on formalin-fixed and paraffin-embedded brain tissues from the following treatment groups: standard diet *Pank2*$^{+/+}$ ($n = 2$); standard diet *Pank2*$^{-/-}$ ($n = 2$); ketogenic diet *Pank2*$^{+/+}$ ($n = 4$); ketogenic diet *Pank2*$^{-/-}$ ($n = 5$); ketogenic diet + pantethine *Pank2*$^{+/+}$ ($n = 3$); ketogenic diet + pantethine *Pank2*$^{-/-}$ ($n = 3$). Briefly, whole formalin-fixed brains were cut in 2-mm thick slices along the sagittal plane, and embedded in formalin. Five to 10-μm thick serial sections were stained with haematoxylin-eosin, periodic acid Schiff, Luxol fast blue and Perls' stain. Immunohistochemistry was performed using antibodies against amyloid precursor protein (Abcam, 1:200), heavy molecular weight neurofilament (Abcam, 1:2000); ubiquitin (Dako, 1:50); phosphorylated tau (Abcam, 1:50), alpha synuclein phospho specific (Covance, 1:200), NeuN (Millipore, 1:500), and glial fibrillary acidic protein (GFAP; Dako, 1:100).

Left quadricep skeletal muscle biopsies were performed in patients according to a protocol approved by the Foundation IRCCS Neurological Institute C. Besta. Morphological analysis in patient and mouse skeletal muscle tissue was carried out on 8 μm cryostat sections using standard histological and histochemical techniques (Dubowitz *et al.* 1973). The reactions for COX and SDH were performed as previously described (Sciacco and Bonilla, 1996). The following treatment groups were analysed: standard diet *Pank2*$^{+/+}$ ($n = 2$); standard diet *Pank2*$^{-/-}$ ($n = 2$); ketogenic diet *Pank2*$^{+/+}$ ($n = 2$); ketogenic diet *Pank2*$^{-/-}$ ($n = 2$); ketogenic diet + pantethine *Pank2*$^{+/+}$ ($n = 2$); and ketogenic diet + pantethine *Pank2*$^{-/-}$ ($n = 2$).

Evaluation of mitochondrial bioenergetics

We analysed mitochondrial energy metabolism in isolated mitochondria derived from brains of standard diet *Pank2*$^{+/+}$ ($n = 3$); standard diet *Pank2*$^{-/-}$ ($n = 3$); standard diet + pantethine *Pank2*$^{+/+}$ ($n = 3$); and standard diet + pantethine *Pank2*$^{-/-}$ ($n = 3$) mice, using an XF96 Extracellular Flux Analyzer (Seahorse Bioscience) as previously reported (Brunetti *et al.*, 2012).

Derivation of neurons from sciatic nerve and analysis of mitochondrial membrane potential

Detection of mitochondrial potential was performed using JC1 staining kit on neurons derived from sciatic nerves isolated from adult mouse as previously described (Brunetti *et al.*, 2012).

Electron microscopy analysis

Sciatic nerve analysis was performed on the following treatment groups: standard diet *Pank2*$^{+/+}$ ($n = 1$); standard diet *Pank2*$^{-/-}$ ($n = 1$); ketogenic diet *Pank2*$^{+/+}$ ($n = 3$); ketogenic diet *Pank2*$^{-/-}$ ($n = 3$); ketogenic diet + pantethine *Pank2*$^{+/+}$ ($n = 3$); and ketogenic diet + pantethine *Pank2*$^{-/-}$ ($n = 3$). Sciatic nerves were surgically removed and processed for epoxy resin embedding as previously described (Brunetti *et al.*, 2012). In particular, each sciatic nerve was cut in proximal, middle and distal segments and dehydrated separately. Ultrastructural analyses were conducted on each stump. Brain ultrastructural analysis was performed on the following treatment groups: standard diet *Pank2*$^{+/+}$ ($n = 1$); standard diet *Pank2*$^{-/-}$ ($n = 1$); ketogenic diet *Pank2*$^{+/+}$ ($n = 3$); ketogenic diet *Pank2*$^{-/-}$ ($n = 3$); ketogenic diet + pantethine *Pank2*$^{+/+}$ ($n = 3$); and ketogenic diet + pantethine *Pank2*$^{-/-}$ ($n = 3$). Sagittally spliced brains were fixed by immersion in glutaraldehyde (2.5% in phosphate buffer). After fixation, serial sagittal slides of 1-mm thick were obtained. Selected areas of interest were sampled, post-fixed in osmium tetroxide and embedded in Epon™ epoxy resin. Thin sections (80–90 nm) were stained with uranyl acetate and lead citrate and examined with a CM10 Philips electron microscope.

Patient and mouse muscle tissues were fixed in 2.5% glutaraldehyde, processed as previously described (Napoli *et al.*, 2011) and post-fixed in 2% osmium tetroxide for 1 h. After dehydration, the specimens were embedded in epoxy resin. Ultrathin sections were cut and stained with uranyl acetate and lead citrate, then examined with a Zeiss electron microscope.

Results

Mice phenotyping

We constantly monitored the weight of *Pank2*$^{+/+}$ and *Pank2*$^{-/-}$ mice during the administration of standard or ketogenic diet. As also previously reported (Kuo *et al.*, 2005) *Pank2*$^{-/-}$ mice under standard diet showed a slight weight reduction as compared with *Pank2*$^{+/+}$ mice, whereas during ketogenic treatment *Pank2*$^{-/-}$ mice showed a fast and progressive weight loss (Fig. 1A and B). Moreover, only *Pank2*$^{-/-}$ mice fed a ketogenic diet manifested kyphosis with hunched position, (Fig. 1C), feet clasping (Fig. 1D), whitening of the fur and rigidity of the tail (Fig. 1E), as well as dystonic limb positioning (Fig. 1F).

We asked whether these signs could have been prevented by pantethine administration. To this aim we treated a group of *Pank2*$^{+/+}$ and *Pank2*$^{-/-}$ mice ('ketogenic diet + pantethine' group) with a ketogenic diet and the concomitant administration of pantethine (15 mg/kg/day) in drinking water. This concentration was established based on a dosage of 900 mg/day in an adult individual ($n = 14$) considering an average weight of 60 kg. We also tested various concentrations of pantethine in mice over 3 weeks and determined that a dose of up to 480 mg/kg/day was tolerated without any side effects on weight and drinking intake (Supplementary Fig. 1).

We observed that, with pantethine administration to mice fed a ketogenic diet, the weight of *Pank2*$^{-/-}$ mice was similar to that of *Pank2*$^{+/+}$ mice (Fig. 1G), no signs of kyphosis or feet clasping were present (Fig. 1H) and body size approached that of *Pank2*$^{-/-}$ mice

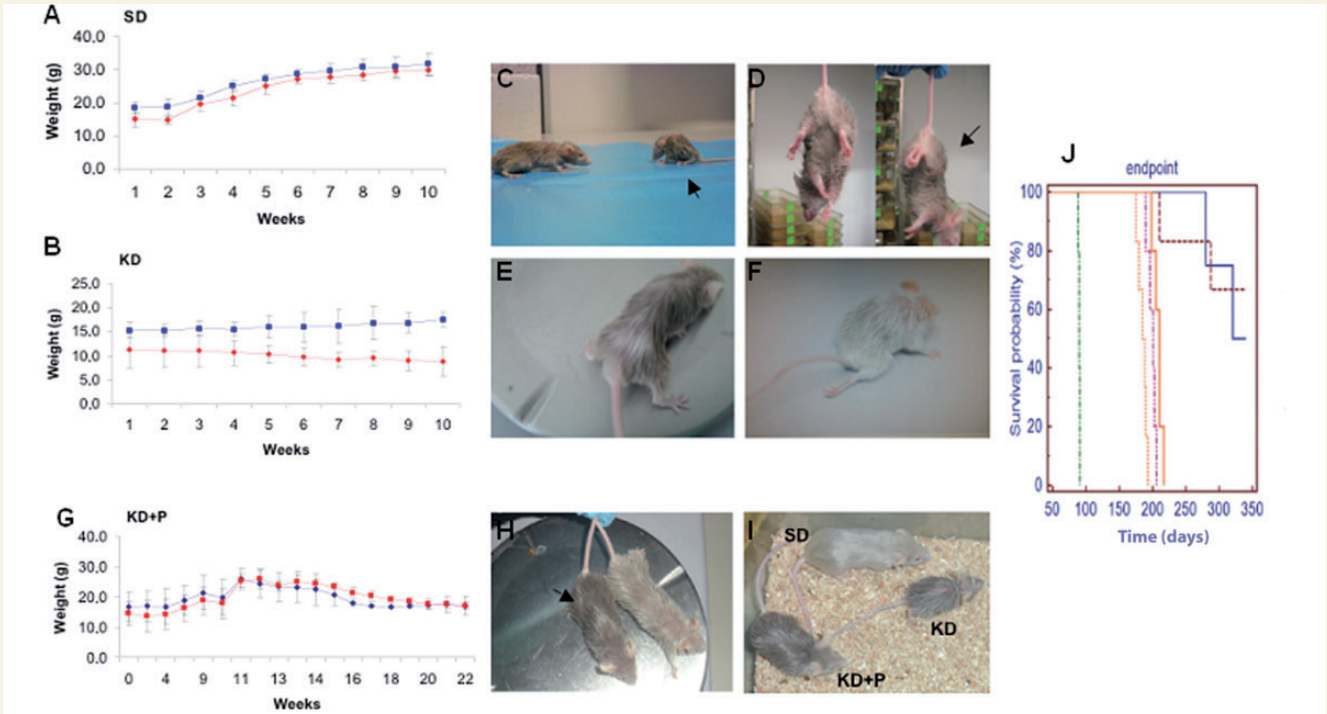

Figure 1 Mice phenotype. (**A**) Body weight of *Pank2*$^{+/+}$ and *Pank2*$^{-/-}$ mice fed a standard diet (SD). (**B**) Body weight of *Pank2*$^{+/+}$ and *Pank2*$^{-/-}$ mice on a ketogenic diet (KD). (**C**) Kyphosis with hunched position; (**D**) feet clasping in ketogenic diet-fed *Pank2*$^{-/-}$ (arrow); (**E**) whitening of the fur and rigidity of the tail in ketogenic diet-fed *Pank2*$^{-/-}$; (**F**) dystonic hindlimb position. (**G**) Body weight of *Pank2*$^{-/-}$ mice was similar to that of *Pank2*$^{+/+}$ fed a ketogenic diet with pantethine administration (KD + P). (**H**) No sign of kyphosis or feet clasping were present in *Pank2*$^{-/-}$ mice on a ketogenic diet with pantethine administration (arrow). (**I**) Comparison of *Pank2*$^{-/-}$ body size in mice on standard (SD), ketogenic (KD) and ketogenic + pantethine (KD + P) diets (**J**) Survival curves for different diet conditions: *Pank2*$^{-/-}$ mice fed a ketogenic diet died after 2 months (dotted green line); *Pank2*$^{+/+}$ mice fed a ketogenic (dotted yellow line); *Pank2*$^{+/+}$ mice fed a ketogenic diet with pantethine (dotted pink line); *Pank2*$^{-/-}$ mice fed a ketogenic diet with pantethine administration prolonged their survival by up to 5 months (orange line); *Pank2*$^{-/-}$ mice fed a standard diet (dotted brown line); and *Pank2*$^{+/+}$ mice fed a standard diet (blue line). In **A**, **B** and **G**, the red symbols indicate *Pank2*$^{-/-}$; blue symbols indicate *Pank2*$^{+/+}$.

fed a standard diet (Fig. 1I). Most importantly, *Pank2*$^{-/-}$ mice fed a ketogenic diet died after 2 months whereas the administration of pantethine prolonged their survival for up to 5 months (Fig. 1J). We could not verify the recovery of retina degeneration as this initial observation (Kuo *et al.*, 2005) was not confirmed by our own investigations and also not reported in another *Pank2* knockout mouse model (Garcia *et al.*, 2012). On the contrary, azoospermia was confirmed in mice fed a standard diet and ketogenic diet but was not rescued by pantethine treatment during the period of our observation and with the dose used.

Motor performance evaluation

Pank2$^{-/-}$ mice fed a ketogenic diet were lethargic and showed a significant reduction of spontaneous movements as compared with *Pank2*$^{+/+}$ mice fed a ketogenic diet, whereas no differences were observed when fed a standard diet (Fig. 2A).

Quantitative motor tests revealed significantly lower activity in *Pank2*$^{-/-}$ mice on a ketogenic diet as compared with *Pank2*$^{+/+}$ mice; no differences were evident on a standard diet (Fig. 2B). The footprint patterns were assessed quantitatively by measuring stride length and hind base width. We found that *Pank2*$^{-/-}$ mice on a ketogenic diet exhibited shorter stride lengths and hind paw width, and an irregular gait as compared with *Pank2*$^{+/+}$ mice on a ketogenic diet (Fig. 2C). All of these abnormalities were recovered by pantethine treatment and *Pank2*$^{-/-}$ mice behaved in the same way as their control littermates (Fig. 2A–C).

Neuropathology of *Pank2*$^{-/-}$ mice fed a ketogenic diet

On histological and immunohistochemical analysis of the whole brains we did not observe massive neural loss, gliosis or demyelination in Pank2$^{-/-}$ mice on a standard diet or a ketogenic diet (data not shown). However, we noticed the presence of small, scattered groups of neurons with eosinophilic, periodic acid Schiff-positive round cytoplasmic inclusions (Fig. 3A–C). These features were observed only in *Pank2*$^{-/-}$ mice on a ketogenic diet, and were located mostly in the midbrain, putamen and amygdala. On immunohistochemistry, the inclusions were sharply positive for ubiquitin (Fig. 3D and F) and negative for amyloid precursor protein, phosphorylated tau, α-synuclein, and high molecular weight neurofilaments (not shown). In addition, ubiquitin

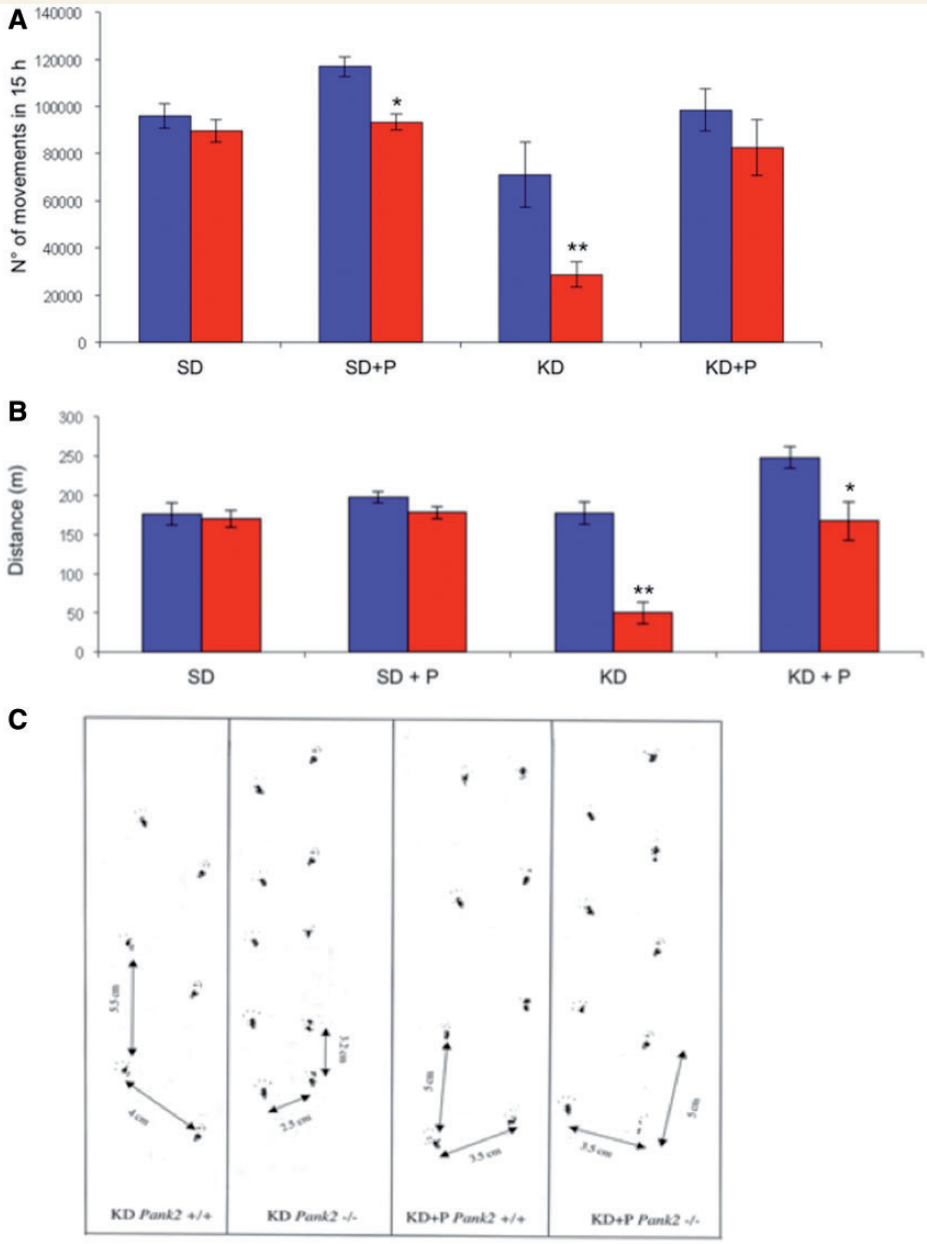

Figure 2 Motor performance evaluation. (**A**) Activity cage: no differences were observed in *Pank2*$^{+/+}$ and *Pank2*$^{-/-}$ mice on a standard diet (SD) or with pantethine (SD + P); *Pank2*$^{+/+}$ mice were more active with pantethine treatment (*$P < 0.05$, two-tailed, unpaired Student's *t*-test). *Pank2*$^{-/-}$ mice fed a ketogenic diet were lethargic and showed a significant reduction of spontaneous movements as compared with *Pank2*$^{+/+}$ mice on a ketogenic diet (**$P < 0.001$, two-tailed, unpaired Student's *t*-test). Pantethine treatment (KD + P) rescues the reduced movements. (**B**) Treadmill test: no differences in the distance travelled by *Pank2*$^{+/+}$ and *Pank2*$^{-/-}$ mice on a standard diet (SD) or with pantethine (SD + P). *Pank2*$^{-/-}$ mice on a ketogenic diet ran only 50 m as compared to 180 m of *Pank2*$^{+/+}$ mice (**$P < 0.001$, two-tailed, unpaired Student's *t*-test). Pantethine treatment (KD + P) restored the running capability in *Pank2*$^{-/-}$ mice and increased the performance in *Pank2*$^{+/+}$ mice (*$P < 0.05$, two-tailed, unpaired Student's *t*-test). (**C**) Footprint pattern: *Pank2*$^{-/-}$ mice fed a ketogenic diet showed shorter stride lengths and hind paw width, and an irregular gait as compared with *Pank2*$^{+/+}$ mice fed a ketogenic diet. Pantethine treatment (KD + P) abolishes the movement disorders. In **A** and **B**, the red bars indicate *Pank2*$^{-/-}$ mice and blue bars indicate *Pank2*$^{+/+}$ mice, respectively.

stain highlighted finely granular cytoplasmic deposits in several neurons, as well as large, ubiquitin positive degenerating neurons (Fig. 3D and E). Iron deposits were not observed with Perl's stain (data not shown).

Pantethine treatment of *Pank2*$^{-/-}$ mice on a ketogenic diet led to the disappearance of neuronal cytoplasmic inclusion on haematoxylin-eosin and periodic acid Schiff stain. Ubiquitin was merely detectable by immunohistochemistry after treatment (Fig. 3G) and

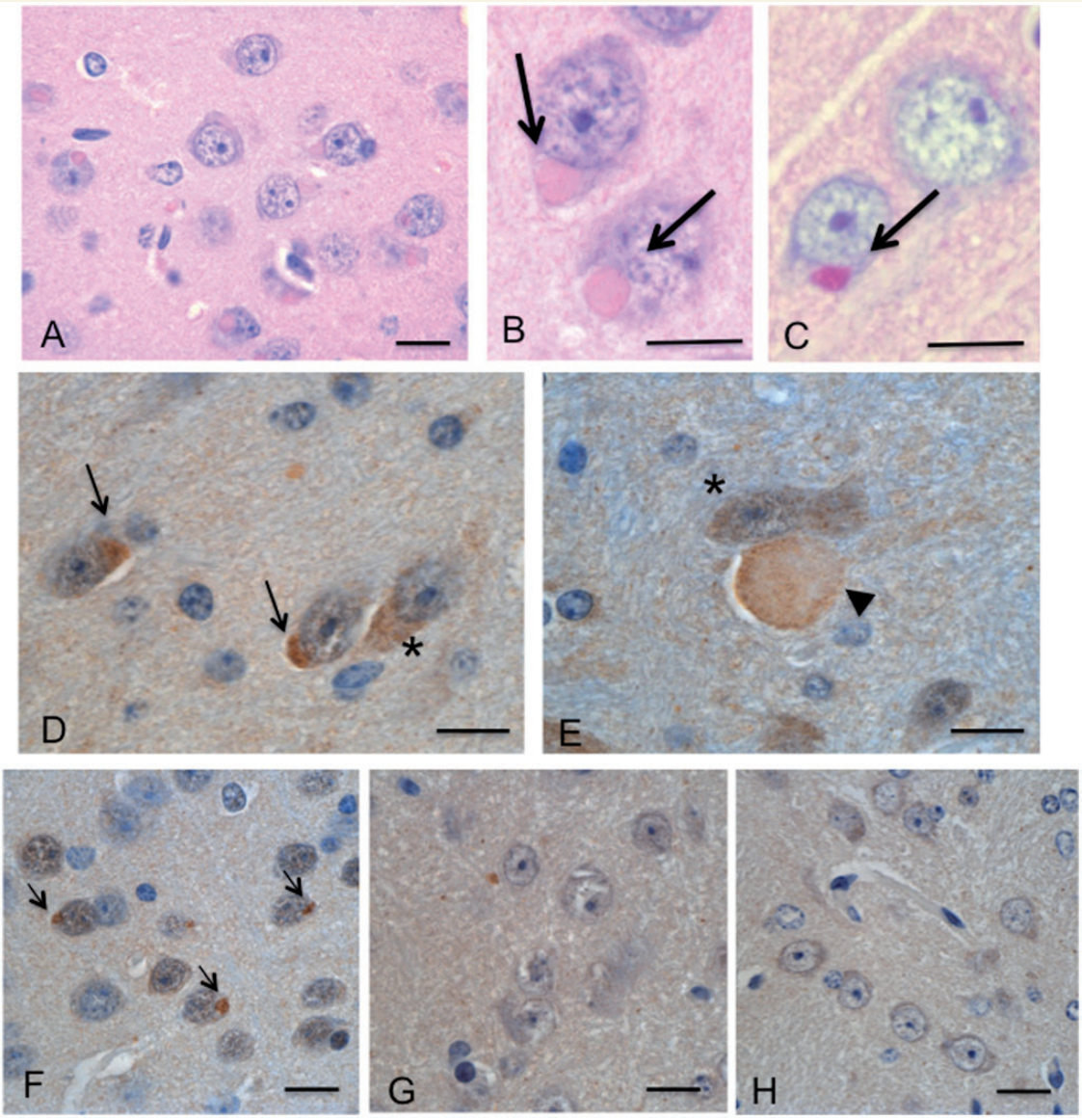

Figure 3 Histology and immunohistochemistry of brains from *Pank2*$^{-/-}$ mice fed a ketogenic diet and a ketogenic diet with pantethine. The analysed animals were 3 months old. Round, eosinophilic, periodic acid Schiff-positive cytoplasmic inclusions were present in neurons of *Pank2*$^{-/-}$ mice fed a ketogenic diet (**A–C**, arrows in **B** and **C**). Cytoplasmic bodies are markedly positive on ubiquitin immunostain (**D** and **F**, arrows). Scattered neurons showed a finely granular cytoplasmic stain for ubiquitin (**D** and **E**, asterisks). There were large degenerating neurons with a diffuse positivity for ubiquitin (**E**, arrowhead). Ubiquitin stain was barely detected in neurons from *Pank2*$^{-/-}$ mice fed a ketogenic diet with pantethine (**G**), which show histological and immunohistochemical features similar to their wild-type littermates (**H**). Scale bars = 25 μm.

completely absent in ketogenic diet-*Pank2*$^{+/+}$ mice brain (Fig. 3H).

Ultrastructural features of central and peripheral nervous systems

Ultrastructural analysis was performed on basal ganglia and peripheral nerve of *Pank2*$^{-/-}$ and *Pank2*$^{+/+}$ mice under different diet conditions. In the basal ganglia, *Pank2*$^{-/-}$ animals on a standard diet showed the presence of numerous mitochondria with abnormal, swollen cristae (Fig. 4). These features were worsened by a ketogenic diet, which led to focal loss of cristae (Fig. 4). *Pank2*$^{-/-}$ animals fed a ketogenic diet also showed cytoplasmic deposits of lipofuscin (data not shown). Notably, pantethine administration completely rescued the mitochondrial morphology of *Pank2*$^{-/-}$ animals on a standard diet, which were indistinguishable from the wild-type littermates (Fig. 4), and ameliorated the morphology of ketogenic diet-fed *Pank2*$^{-/-}$ mice (Fig. 4).

Ultrastructural analysis of peripheral nerve of *Pank2*$^{-/-}$ animals on a ketogenic diet showed the presence of swollen mitochondria, characterized by cristae degeneration and by the presence of amorphous material in the matrix (Fig. 5). Pantethine

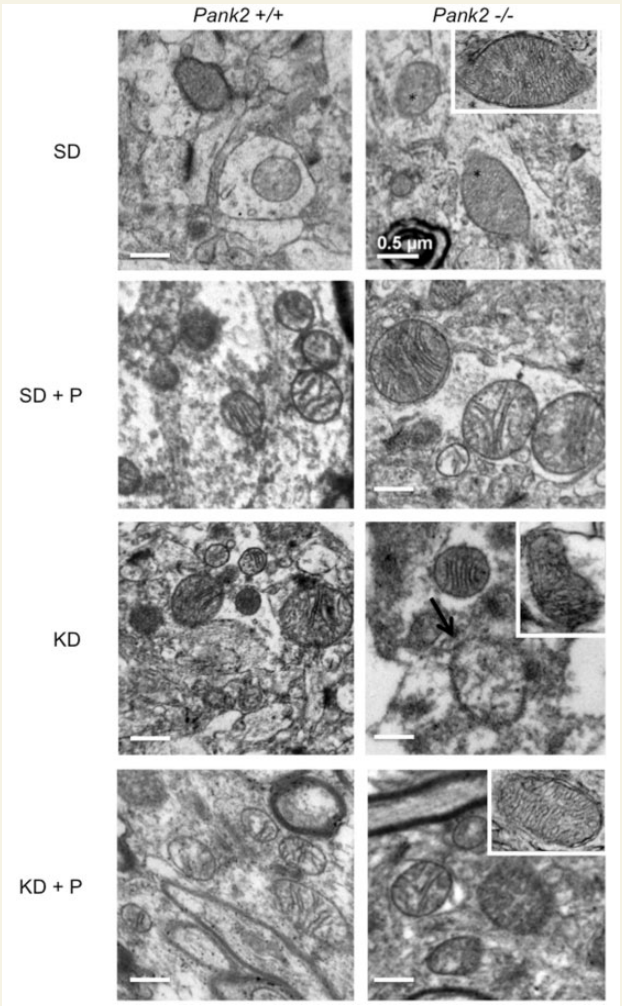

Figure 4 Electron microscopy of basal ganglia in *Pank2*$^{+/+}$ and *Pank2*$^{-/-}$ mice under different diet conditions. The analysed animals were 3 months old. *Pank2*$^{+/+}$ mice on a standard diet (SD), a standard diet + pantethine (SD + P), ketogenic diet (KD) and ketogenic diet + pantethine (KD + P) show normal mitochondria. *Pank2*$^{-/-}$ mice on a standard diet show mitochondria with swollen cristae (asterisks and insert). With a ketogenic diet the mitochondrial morphology is worsened with focal loss of cristae (arrow and insert). *Pank2*$^{-/-}$ mice on standard diet with pantethine were similar to wild-type littermates; with a ketogenic diet with pantethine there is a prevalence of mitochondria with normal cristae morphology, although a few mitochondria still showed swollen cristae.

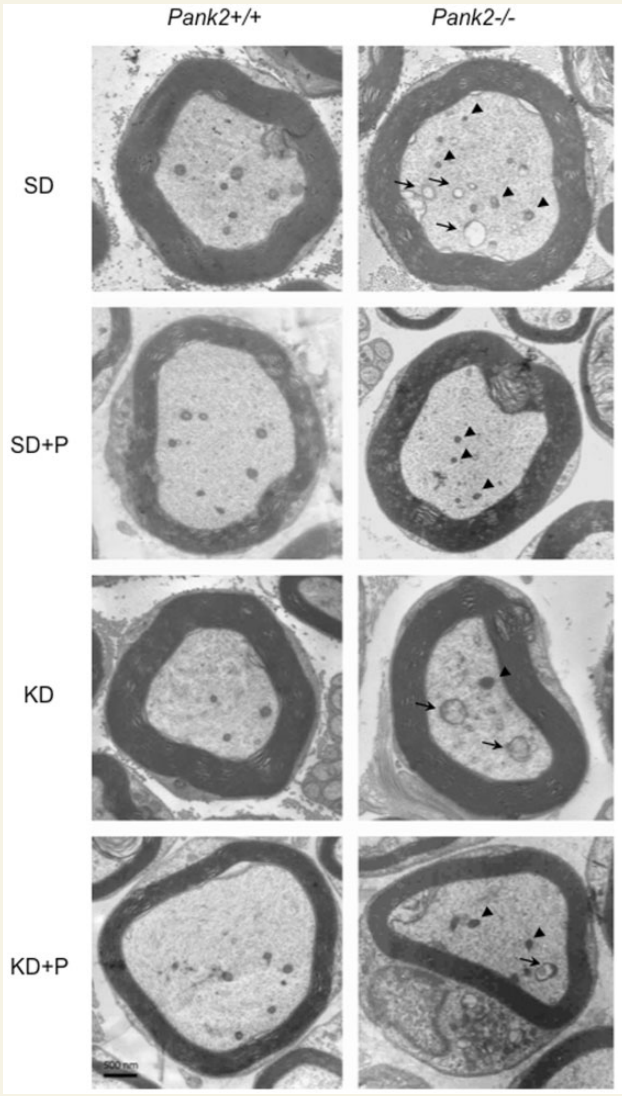

Figure 5 Electron microscopy of peripheral nerve in *Pank2*$^{+/+}$ and *Pank2*$^{-/-}$ mice under different diet conditions. The analysed animals were 3 months old. Sciatic nerve axons of *Pank2*$^{+/+}$ mice on a standard diet (SD), standard diet + pantethine (SD + P), ketogenic diet (KD) and ketogenic diet + pantethine (KD + P) contain morphologically normal mitochondria. Sciatic nerve axons of *Pank2*$^{-/-}$ mice on a standard diet and ketogenic diet show swollen mitochondria with altered cristae (arrows). Sciatic nerve axons of *Pank2*$^{-/-}$ mice on a standard diet + pantethine and ketogenic diet + pantethine show a high prevalence of normally-shaped mitochondria with regular cristae organization (arrowheads). Scale bars = 500 µm.

administration was able to completely rescue the mitochondrial morphology both in the PNS and CNS. No ultrastructural alterations were observed in *Pank2*$^{+/+}$ mice fed with standard or ketogenic diets (Figs 4 and 5).

Pantethine restores mitochondrial membrane potential of *Pank2*$^{-/-}$ neurons

To evaluate mitochondrial membrane potential we used JC1 staining. As shown in Fig. 6, neurons derived from *Pank2*$^{+/+}$ animals treated with a standard or ketogenic diet presented red fluorescent aggregates indicating the preservation of the mitochondrial membrane potential. On the contrary, neurons derived from *Pank2*$^{-/-}$ mice treated with a standard or ketogenic diet presented with a diffuse green fluorescence (Fig. 6) confirming the presence of a defective mitochondrial membrane potential. Interestingly, neurons derived from *Pank2*$^{-/-}$ mice under

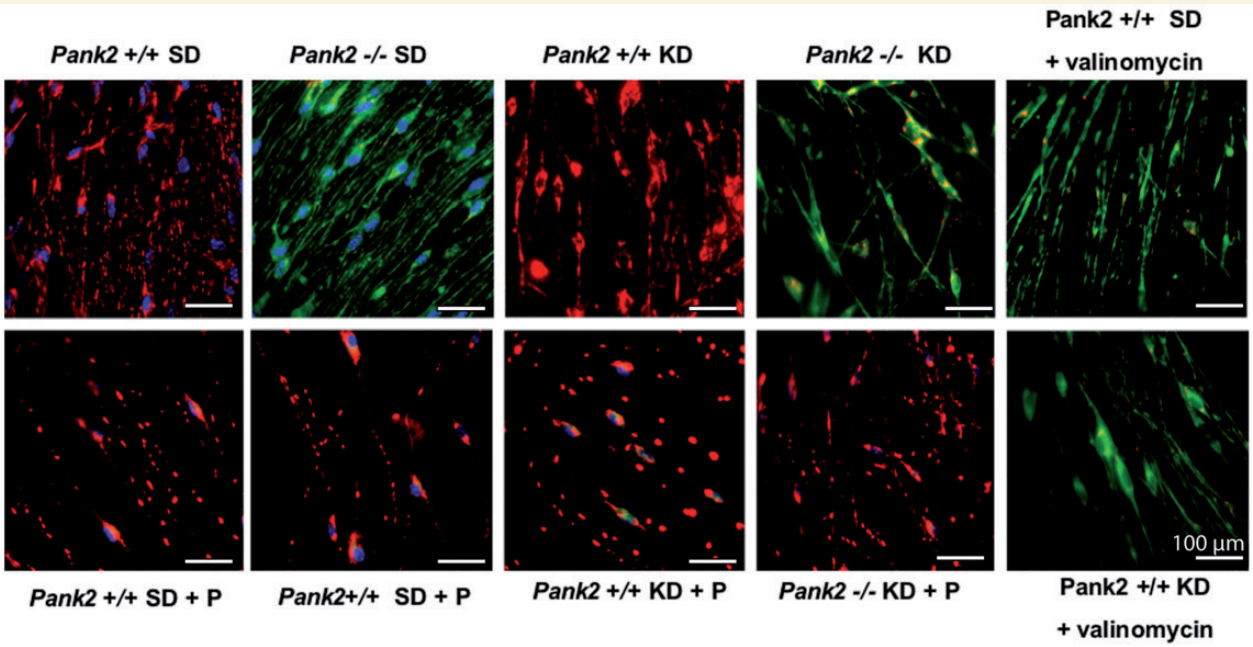

Figure 6 Membrane potential in *Pank2*$^{+/+}$ and *Pank2*$^{-/-}$ neurons derived from mice under different diet conditions. Neurons derived from *Pank2*$^{+/+}$ animals treated with a standard (SD) or ketogenic diet (KD), with or without pantethine (P) presented red fluorescent aggregates indicating the preservation of the mitochondrial membrane potential. Neurons derived from *Pank2*$^{-/-}$ mice treated with a standard or ketogenic diet presented with a diffuse green fluorescence confirming the presence of a defective mitochondrial membrane potential. Neurons derived from *Pank2*$^{-/-}$ mice with standard and ketogenic treatment plus the addition of pantethine, showed predominantly red fluorescence aggregates, indicating preservation of mitochondrial membrane potential. Scale bars = 100 µm.

standard and ketogenic treatment plus the addition of pantethine in drinking water, showed predominantly red fluorescence aggregates indicating that the mitochondrial membrane potential was preserved.

Pantethine improves mitochondrial respiration

We evaluated respiration with microscale oxygraphy on mitochondria isolated from brains of *Pank2*$^{+/+}$ and *Pank2*$^{-/-}$ mice treated with pantethine and we compared the results with untreated mice. Measurement was not performed in mitochondria derived from mice under ketogenic treatment because of technical difficulties, probably due to the presence of increased fat levels in the brain. We measured basal oxygen consumption rate, and oxygen consumption rate after ADP addition, and after oligomycin addition. We observed that pantethine was able to significantly increase oxygen consumption rate under all conditions tested in both *Pank2*$^{+/+}$ and *Pank2*$^{-/-}$ mitochondria (Fig. 7). In particular, pantethine determines a doubling in oxygen consumption rate after ADP stimulation suggesting a tightly coupled respiration with ATP production.

These differences were statistically significant as demonstrated by an unpaired, two-sided Student's *t*-test, assuming unequal variance. Values for statistical significance were set at $P < 0.05$.

Comparison of muscle derived from *Pank2*$^{-/-}$ mice on a ketogenic diet versus a patient with pantothenate kinase-associated neurodegeneration

COX histochemical reaction of the muscle derived from *Pank2*$^{-/-}$ mice fed a ketogenic diet revealed a peculiar staining pattern, likely because of the presence of abnormal mitochondria (Fig. 8A). We had the opportunity to study the muscle biopsy of a 6-year-old patient with PKAN (*PANK2* mutations: N500I + IVS2-1G > A). We did not observe any defects in the respiratory chain enzymatic activities apart from a succinate dehydrogenase (SDH) activity below the lower control value (not shown), but we found the same COX staining pattern (Fig. 8B) observed in mice. To characterize these mitochondria further we performed electron microscopy, which highlighted the presence of giant mitochondria spanning the sarcomere between two neighbouring Z-lines and showing irregularly shaped cristae (Fig. 8C).

The histological alterations of the *Pank2*$^{-/-}$ muscle highlighted by both trichrome and COX staining were absent in pantethine-treated mice (Fig. 9). Moreover, no histological abnormalities were evident in standard diet or ketogenic diet *Pank2*$^{+/+}$ muscle (Fig. 9).

Plasma analysis

Plasma analysis showed an increase of cholesterol (Supplementary Fig. 2A) and triglycerides (Supplementary Fig. 2B) in mice on a

ketogenic diet. As expected, pantethine was able to reduce the levels of both (Supplementary Fig. 2A and B). A decrease of glucose levels was detected in mice fed a ketogenic diet and a ketogenic + pantethine diet (Supplementary Fig. 2C). Ketosis was observed in mice fed a ketogenic diet and was maintained during pantethine administration (Supplementary Fig. 2D).

Discussion

The *Pank2*$^{-/-}$ mouse model did not recapitulate the clinical and neuropathological features of the human condition (Kuo *et al.*, 2005; Brunetti *et al.*, 2012). Based on the role of co-enzyme A in several crucial metabolic pathways and considering the data obtained by a metabolomics approach in patients with PKAN, indicating the presence of impairment in lipid metabolism, we tested the hypothesis to challenge this mouse model with a diet containing high fat levels. Ketogenic diet consists of a low glucose and high lipid content, stimulating lipid use by mitochondrial beta-oxidation and ketone body production in the liver. Ketone bodies are high-energy-content compounds that can be used as an energy source by the brain, heart and skeletal muscle. We administered a low carbohydrate high-fat ketogenic diet to 2-month-old *Pank2*$^{-/-}$ and *Pank2*$^{+/+}$ mice and evaluated the clinical and biochemical phenotype.

We demonstrate here that the introduction of the ketogenic diet resulted in the onset of a severe phenotype in *Pank2*$^{-/-}$ mice characterized by motor dysfunctions, neurological impairment with feet-clasping, and exacerbated mitochondrial alterations, which were also present in the brain and PNSs of 12-month-old *Pank2*$^{-/-}$ mice on a standard diet (Brunetti *et al.*, 2012). Moreover, this diet caused the premature death of *Pank2*$^{-/-}$ mice.

Pank2$^{-/-}$ mice fed a ketogenic diet did show the clinical signs present in patients with PKAN, namely more severe movement disorder and neurodegeneration. Importantly, these animals showed histological and immunohistochemical features of neurodegeneration, with cytoplasmic accumulation of abnormal, ubiquinated proteins as observed in the brains of patients with PKAN (Kruer *et al.*, 2011). However, the exact nature of the ubiquitinated proteins in our model remains to be elucidated. As observed in humans, cytoplasmic inclusions in *Pank2*$^{-/-}$ mice were negative for α-synuclein, confirming that PKAN neuropathological findings are different from other forms of neurodegeneration with brain iron accumulation.

We did not observe iron accumulation in *Pank2*$^{-/-}$ mice on a ketogenic diet, in contrast to that observed in human PKAN brains. We cannot exclude that iron levels could be below the detection level for the histological technique or that iron accumulates over a period of time beyond our observation. These aspects are still to be clarified and require further investigation.

The induction of a PKAN-like phenotype in *Pank2*$^{-/-}$ mice fed with a ketogenic diet, allowed us to have a model in which to test therapeutic compounds. Recently, in the *Drosophila* dPANK/*fbl* mutants it was shown that panthethine can work as a precursor of co-enzyme A, even in the presence of severely reduced levels of

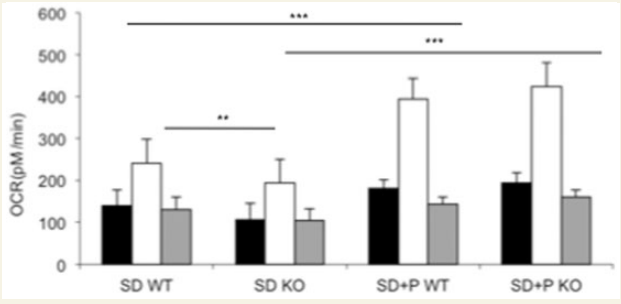

Figure 7 Evaluation of mitochondrial bioenergetics status. Oxygen consumption rate (OCR) in mitochondria isolated from brains of *Pank2*$^{+/+}$ and *Pank2*$^{-/-}$ mice treated with pantethine and compared with untreated mice. We measured basal oxygen consumption rate (OCR-B) after ADP addition (OCR-ADP), and after oligomycin addition (OCR-O). Pantethine was able to significantly increase oxygen consumption rate in both *Pank2*$^{+/+}$ and *Pank2*$^{-/-}$ mitochondria, especially ADP-induced respiration. Black, white and grey histograms indicate OCR-B, -ADP, and -O, respectively. Bars indicate the standard deviation (SD). $^{**}P < 0.01$; *** $P < 0.001$ (unpaired, two-tail Student's *t*-test). WT = wild-type; KO = knock-out.

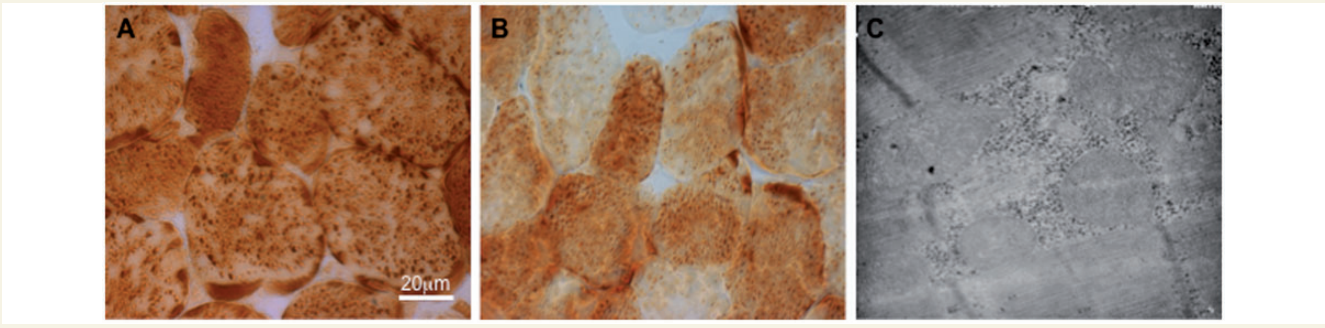

Figure 8 Muscle COX (cytochrome *c* oxidase) histochemical reaction and electron microscopy. (**A**) *Pank2*$^{-/-}$ mice on a ketogenic diet. (**B**) Patient with PKAN revealed the same peculiar staining pattern as mice fed a ketogenic diet. (**C**) Electron microscopy highlighted the presence of giant mitochondria spanning the sarcomere between two neighbouring Z-lines and showing irregularly shaped cristae ($\times$20 000).

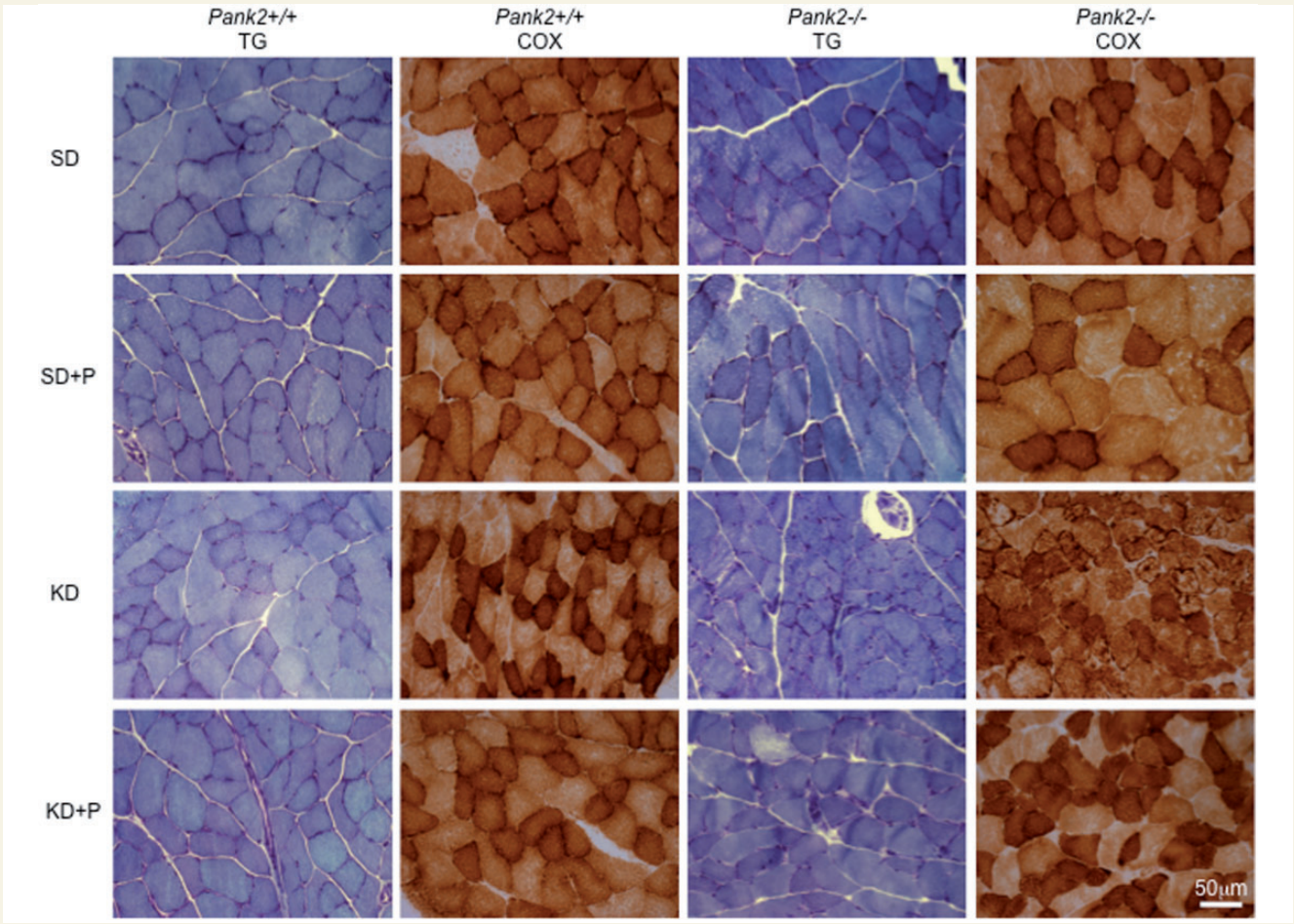

Figure 9 Gomori trichrome (TG) and COX histochemical reactions in muscle of *Pank2*$^{+/+}$ and *Pank2*$^{-/-}$ mice under different diet conditions. No alterations were present in *Pank2*$^{+/+}$ mice. Ketogenic diet (KD) induced muscle histological abnormalities in *Pank2*$^{-/-}$ mice (see also Fig. 8A) characterized by the presence of enlarged mitochondria. These alterations were rescued by pantethine administration (KD + P). Magnification × 400. SD = standard diet.

functional pantothenate kinase and that it was able to rescue brain degeneration, mitochondrial dysfunction and locomotor disabilities (Rana *et al.*, 2010). By reasoning on these data we decided to administer pantethine to mice under ketogenic treatment and, as an internal control, to mice on a standard diet. In *Pank2*$^{-/-}$ mice on a ketogenic diet, we observed the rescue of the clinical phenotype including the movement disorder, the amelioration of the mitochondrial dysfunctions, and the extension of the lifespan as previously demonstrated in *Drosophila* (Rana *et al.*, 2010). Treatment with pantethine dramatically improved both the histological features of neurodegeneration and the ultrastructural mitochondrial damage in *Pank2*$^{-/-}$ mice fed a ketogenic diet. We did not observe rescue of the azoospermic phenotype in mice. Fertility was not thoroughly investigated in patients with PKAN because of the severity of their clinical presentation and shortened lifespan. However, analysis of sperm samples in two affected individuals showed aberrant morphology and altered motility (Gregory and Hayflick, 2005).

We also demonstrated that pantethine administration was able to rescue the mitochondrial phenotype in neurons derived from *Pank2*$^{-/-}$ mice on a standard diet, indicating that its effectiveness was not dependent on or influenced by the ketogenic treatment. It is known that pantethine is rapidly converted into cysteamine and pantothenate by the vanin enzyme, also known as pantetheine hydrolase or pantetheinase (Kaskow *et al.*, 2012). Although pantethine is not able to cross the blood–brain barrier, Bousquet *et al.* (2010) demonstrated that cysteamine can cross the blood–brain barrier and in so doing can exert positive effects on the striatum and substantia nigra (Gibrat and Cicchetti, 2011). Cysteamine is able to enhance the expression of tyrosine hydroxylase protein and of the *Nurr1* gene (now known as *Nr4a2*), and to upregulate the expression of the Brain Derived Neurotrophic Factor (BDNF). These neuroprotective effects of cysteamine and of its dimer cystamine have been hypothesized to reflect the positive actions of this compound in Parkinson's disease (Sun *et al.*, 2010; Gibrat and Cicchetti, 2011) and Huntington's disease (Borrell-Pages *et al.*, 2006).

It has been observed that cysteamine and pantethine in drinking water have beneficial effects in MPTP-induced mouse models of Parkinson's disease (Cornille *et al.*, 2010; Sun *et al.*, 2010) and

would prevent neuronal degeneration in animal models of Parkinson's disease (Stack *et al.*, 2008; Gibrat and Cicchetti, 2011). Moreover, in animal models of Huntington's disease, cysteamine exerts its neuroprotective effects by prolonging lifespan and decreasing motor symptoms (Dedeoglu *et al.*, 2002; Karpuj *et al.*, 2002).

In agreement with these data, we can hypothesize that the beneficial effects of pantethine in our model system were due to its conversion into pantothenate and cysteamine. In fact, pantethine is rapidly hydrolyzed to pantothenic acid and cysteamine as it could not be detected in plasma after oral administration (Wittwer *et al.*, 1985). Cysteamine, the reduced form of cystamine (2-aminoethanethiol) is approved by the FDA for the treatment of cystinosis, a childhood disorder, which causes renal failure through cystine intracellular accumulation (Dohil *et al.*, 2010) and in 2006 a small trial with this compound was initiated in patients with Huntington's disease (Dohil *et al.*, 2010).

However, cysteamine causes side effects (Corden *et al.*, 1981) whereas pantethine has low toxicity (Knott *et al.*, 1957; Schwartz and Bagdon, 1964) and might act as a neutral systemic carrier that would target cysteamine into the brain, avoiding toxicity and maximizing its efficacy.

The metabolism of cysteamine generates several intermediates including hypotaurine and taurine. In addition to being the major bile salt, in the form of taurocholate (Bouckenooghe *et al.*, 2006), taurine crosses the blood–brain barrier and is involved in brain physiological activities such as inhibitory neurotransmission and long-term potentiation (Muramatsu *et al.*, 1978; Pasantes-Morales *et al.*, 1981). Recently, we observed a reduction of the bile acids tauro and glycol cholate (Leoni *et al.*, 2012) and an alteration of lipid metabolism in plasma derived from patients with PKAN, likely because of co-enzyme A shortage causing, among others, dysfunctional fat assimilation.

Together with the data obtained in mice fed a high-fat diet, these observations suggest that it is possible to trace a parallel between patients with PKAN and *Pank2*$^{-/-}$ mice under stressful conditions. Moreover, it is important to consider that environmental factors, such as food intake, together with genetic background could modulate the disease presentation by worsening or, on the contrary, stabilizing the progression of the symptoms. This could also explain the variability of the clinical presentation of the disease, with a spectrum of syndromes ranging from rapid to slowly progressive.

Interestingly, we have analysed for the first time the muscle histology of a genetically defined patient with PKAN. The first neuromuscular examination was performed by Malandrini *et al.* (1995) in two adult cases of clinically-defined Hallerworden-Spatz disease, which showed the presence of subsarcolemmal myeloid structures, features characteristic of inflammatory myopathies.

In our study we demonstrated that the muscle of a 6-year-old patient with PKAN showed giant mitochondria with a mild alteration of the cristae and was histologically comparable with the muscle of *Pank2*$^{-/-}$ mice fed a ketogenic diet. These alterations were rescued in mice after pantethine administration. This is a relevant observation when considering the option of pantethine administration to patients, as muscle analysis could represent the quantitative read-out to evaluate the effect of the compound with a minimal invasive procedure.

Taken together, these data strongly suggest that pantethine administration to patients with PKAN should be considered as a possible, safe and non-toxic therapeutic approach. Moreover, our data clearly demonstrate that an altered lipid metabolism, as a result of co-enzyme A shortage, could represent one of the underlining causes of the disease. It is also possible, as demonstrated by the presence of mitochondrial alteration in the mouse model and in the muscle of a patient with PKAN, that mitochondria play a relevant role or could be a concurrent cause in the pathogenic mechanism of the disease. Interestingly, the presence of giant mitochondria in muscle, although with slight morphological differences, resembles the picture present in another human disorder caused by mutations in the *CHKB* gene and mainly characterized by muscular dystrophy and mental retardation (Quinlivan *et al.*, 2013). *CHKB* encodes an enzyme catalysing the first step in *de novo* phosphatidylcholine synthesis (Mitsuhashi *et al.*, 2013). CHKB and PANK2 are clearly part of different metabolic pathways but they converge on phospholipid biosynthesis. It is tempting to speculate that dysfunction of lipid metabolism is indeed the common culprit of the generation of mitochondrial muscle alteration observed in both disorders (Lamari *et al.*, 2013).

We believe that the modulation of the diet composition in *Pank2* knockout mice has generated a useful model system in which to test not only pantethine, but also additional compounds, which could be beneficial for patients.

Acknowledgements

We would like to thank Stefano D'Arrigo for the clinical data of the patient with PKAN. A special thank to Emilio Ciusani, Stefania Saccucci and Anil Rana for technical support.

Funding

The financial support of Telethon GGP11088 to V.T. is gratefully acknowledged. This work was supported by TIRCON project of the European Commission's Seventh Framework Programme (FP7/2007-2013, HEALTH-F2-2011, grant agreement No. 277984).

Supplementary material

Supplementary material is available at *Brain* online.

References

Borrell-Pages M, Canals JM, Cordelieres FP, Parker JA, Pineda JR, Grange G, et al. Cystamine and cysteamine increase brain levels of BDNF in Huntington disease via HSJ1b and transglutaminase. J Clin Invest 2006; 116: 1410–24.

Bouckenooghe T, Remacle C, Reusens B. Is taurine a functional nutrient? Curr Opin Clin Nutr Metab Care 2006; 9: 728–33.

Bousquet M, Gibrat C, Ouellet M, Rouillard C, Calon F, Cicchetti F. Cystamine metabolism and brain transport properties: clinical

implications for neurodegenerative diseases. J Neurochem 2010; 114: 1651–8.
Brunetti D, Dusi S, Morbin M, Uggetti A, Moda F, D'Amato I, et al. Pantothenate kinase-associated neurodegeneration: altered mitochondria membrane potential and defective respiration in Pank2 knock-out mouse model. Hum Mol Genet 2012; 21: 5294–305.
Corden BJ, Schulman JD, Schneider JA, Thoene JG. Adverse reactions to oral cysteamine use in nephropathic cystinosis. Dev Pharmacol Ther 1981; 3: 25–30.
Cornille E, Abou-Hamdan M, Khrestchatisky M, Nieoullon A, de Reggi M, Gharib B. Enhancement of L-3-hydroxybutyryl-CoA dehydrogenase activity and circulating ketone body levels by pantethine. Relevance to dopaminergic injury. BMC Neurosci 2010; 11: 51.
Dedeoglu A, Kubilus JK, Jeitner TM, Matson SA, Bogdanov M, Kowall NW, et al. Therapeutic effects of cystamine in a murine model of Huntington's disease. J Neurosci 2002; 22: 8942–50.
Dohil R, Fidler M, Gangoiti JA, Kaskel F, Schneider JA, Barshop BA. Twice-daily cysteamine bitartrate therapy for children with cystinosis. J Pediatr 2010; 156: 71–5e1–3.
Dubowitz V, Brooke MH. Muscle biopsy: a modern approach. London; Philadelphia, USA: Sanders; 1973.
Garcia M, Leonardi R, Zhang YM, Rehg JE, Jackowski S. Germline deletion of pantothenate kinases 1 and 2 reveals the key roles for CoA in postnatal metabolism. PLoS One 2012; 7: e40871.
Gibrat C, Cicchetti F. Potential of cystamine and cysteamine in the treatment of neurodegenerative diseases. Prog Neuropsychopharmacol Biol Psychiatry 2011; 35: 380–9.
Gregory A, Hayflick SJ. Neurodegeneration with brain iron accumulation. Folia Neuropathol 2005; 43: 286–96.
Gregory A, Polster BJ, Hayflick SJ. Clinical and genetic delineation of neurodegeneration with brain iron accumulation. J Med Genet 2009; 46: 73–80.
Gregory A, Westaway SK, Holm IE, Kotzbauer PT, Hogarth P, Sonek S, et al. Neurodegeneration associated with genetic defects in phospholipase A(2). Neurology 2008; 71: 1402–9.
Hayflick SJ. Pantothenate kinase-associated neurodegeneration (formerly Hallervorden-Spatz syndrome). J Neurol Sci 2003; 207: 106–7.
Hayflick SJ, Westaway SK, Levinson B, Zhou B, Johnson MA, Ching KH, et al. Genetic, clinical, and radiographic delineation of Hallervorden-Spatz syndrome. N Engl J Med 2003; 348: 33–40.
Karpuj MV, Becher MW, Springer JE, Chabas D, Youssef S, Pedotti R, et al. Prolonged survival and decreased abnormal movements in transgenic model of Huntington disease, with administration of the transglutaminase inhibitor cystamine. Nat Med 2002; 8: 143–9.
Kaskow BJ, Proffitt JM, Blangero J, Moses EK, Abraham LJ. Diverse biological activities of the vascular non-inflammatory molecules—the Vanin pantetheinases. Biochem Biophys Res Commun 2012; 417: 653–8.
Knott RP, Tsao DP, McCutcheon RS, Cheldelin VH, King TE. Toxicity of pantetheine. Proc Soc Exp Biol Med 1957; 95: 340–1.
Kruer MC, Boddaert N, Schneider SA, Houlden H, Bhatia KP, Gregory A, et al. Neuroimaging features of neurodegeneration with brain iron accumulation. Am J Neuroradiol 2012; 33: 407–14.
Kruer MC, Hiken M, Gregory A, Malandrini A, Clark D, Hogarth P, et al. Novel histopathologic findings in molecularly-confirmed pantothenate kinase-associated neurodegeneration. Brain 2011; 134 (Pt 4): 947–58.
Kuo YM, Duncan JL, Westaway SK, Yang H, Nune G, Xu EY, et al. Deficiency of pantothenate kinase 2 (Pank2) in mice leads to retinal degeneration and azoospermia. Hum Mol Genet 2005; 14: 49–57.
Kuo YM, Hayflick SJ, Gitschier J. Deprivation of pantothenic acid elicits a movement disorder and azoospermia in a mouse model of pantothenate kinase-associated neurodegeneration. J Inherit Metab Dis 2007; 30: 310–7.
Laffel L. Ketone bodies: a review of physiology, pathophysiology and application of monitoring to diabetes. Diabetes Metab Res Rev 1999; 15: 412–26.
Lamari F, Mochel F, Sedel F, Saudubray JM. Disorders of phospholipids, sphingolipids and fatty acids biosynthesis: toward a new category of inherited metabolic diseases. J Inherit Metab Dis 2013; 36: 411–25.
Leonardi R, Rehg JE, Rock CO, Jackowski S. Pantothenate kinase 1 is required to support the metabolic transition from the fed to the fasted state. PLoS One 2010; 5: e11107.
Leonardi R, Rock CO, Jackowski S, Zhang YM. Activation of human mitochondrial pantothenate kinase 2 by palmitoylcarnitine. Proc Natl Acad Sci USA 2007; 104: 1494–9.
Leoni V, Strittmatter L, Zorzi G, Zibordi F, Dusi S, Garavaglia B, et al. Metabolic consequences of mitochondrial coenzyme A deficiency in patients with PANK2 mutations. Mol Genet Metab 2012; 105: 463–71.
Malandrini A, Bonuccelli U, Parrotta E, Ceravolo R, Berti G, Guazzi GC. Myopathic involvement in two cases of Hallervorden-Spatz disease. Brain Dev 1995; 17: 286–90.
Mitsuhashi S, Nishino I. Megaconial congenital muscular dystrophy due to loss-of-function mutations in choline kinase β. Curr Opin Neurol 2013; 26: 536–43.
Muramatsu M, Kakita K, Nakagawa K, Kuriyama K. A modulating role of taurine on release of acetylcholine and norepinephrine from neuronal tissues. Jpn J Pharmacol 1978; 28: 259–68.
Napoli L, Crugnola V, Lamperti C, Silani V, Di Mauro S, Bresolin N, et al. Ultrastructural mitochondrial abnormalities in patients with sporadic amyotrophic lateral sclerosis. Arch Neurol 2011; 68: 1612–3.
Pasantes-Morales H, Chaparro H, Otero E. Clinical study on the effect of taurine on intractable epileptics (author's transl). Rev Invest Clin 1981; 33: 373–8.
Quinlivan R, Mitsuahashi S, Sewry C, Cirak S, Aoyama C, Mooore D, et al. Muscular dystrophy with large mitochondria associated with mutations in the CHKB gene in three British patients: extending the clinical and pathological phenotype. Neuromuscul Disord 2013; 23: 549–56.
Rana A, Seinen E, Siudeja K, Muntendam R, Srinivasan B, van der Want JJ, et al. Pantethine rescues a Drosophila model for pantothenate kinase-associated neurodegeneration. Proc Natl Acad Sci USA 2010; 107: 6988–93.
Schwartz E, Bagdon RE. Toxicity studies of some derivatives of pantothenic acid. Toxicol Appl Pharmacol 1964; 6: 280–3.
Sciacco M, Bonilla E. Cytochemistry and immunocytochemistry of mitochondria in tissue sections. Methods Enzymol 1996; 264: 509–21.
Stack EC, Ferro JL, Kim J, Del Signore SJ, Goodrich S, Matson S, et al. Therapeutic attenuation of mitochondrial dysfunction and oxidative stress in neurotoxin models of Parkinson's disease. Biochim Biophys Acta 2008; 1782: 151–62.
Sun L, Xu S, Zhou M, Wang C, Wu Y, Chan P. Effects of cysteamine on MPTP-induced dopaminergic neurodegeneration in mice. Brain Res 2010; 1335: 74–82.
Wittwer CT, Gahl WA, Butler JD, Zatz M, Thoene JG. Metabolism of pantethine in cystinosis. J Clin Invest 1985; 76: 1665–72.